



Infrared Reflection Spectroscopy and Effective Medium Modeling of As-Anodized and Oxidized Porous Silicon Carbide

JONATHAN E. SPANIER AND IRVING P. HERMAN

Department of Applied Physics, Columbia Radiation Laboratory, Columbia University, New York, NY 10027, USA

Abstract. We present a study of the infrared reflectance of porous silicon carbide (PSC) formed by the electrochemical dissolution of silicon carbide substrates of both 6H and 4H polytypes. The reflectance from *n*-PSC, both as-anodized and passivated, is reported for the first time. The passivation of PSC has been accomplished using a short thermal oxidation. Fourier transform infrared (FTIR) reflectance spectroscopy is employed *ex situ* after different stages of the thermal oxidation process. The characteristics of the reststrahlen band normally observed in bulk SiC are altered by anodization; further changes in the reflectance spectra occur following oxidation for different periods of time. An effective medium theory model that includes air, SiC and SiO₂ as component materials is shown to characterize the observed changes in the reflectance spectra after different stages of PSC oxidation.

Keywords: porous silicon carbide, oxidation, effective medium theory, infrared reflectance (or IR), reststrahlen

I. Introduction

The passivation of porous semiconductors by short-term oxidation has been shown to enhance the radiative efficiency of the porous material, increase its structural stability and resistance to further oxidation, and, in some cases, shorten the wavelength of the luminescence spectrum [1]. Porous silicon carbide (PSC) has been of interest recently because it photoluminescences more efficiently than bulk SiC. The thermal oxidation of PSC has been shown to enhance the photoluminescence efficiency markedly and shorten the PL wavelength *vis-à-vis* as-anodized PSC and bulk SiC [2]. Also, PSC oxidizes more slowly under ambient conditions than porous silicon (PS). Therefore, changes in the PSC properties due to high-temperature thermal oxidation can be distinguished more easily from those changes that are due to aging in ambient alone, which permits a well-controlled study of oxide passivation of a porous semiconductor.

Fourier transform infrared (FTIR) reflectance has been used to investigate the nanostructure of PSC nondestructively [3]. As a partially ionic lattice, SiC exhibits nondegenerate longitudinal optical (LO) and transverse optical (TO) phonons in the far infrared

portion of the spectrum. The *reststrahlen* band, which is the high reflectance between the TO and LO phonon frequencies, is shown for bulk SiC as the solid line in Fig. 1. The dashed line denoted by “as-anodized” in Fig. 1 shows the measured *reststrahlen* band in a typical PSC film, which is substantially different than that in bulk SiC. The splitting of the *reststrahl* band in the reflectance from PSC is likely due to surface phonons and the appearance of a pronounced peak at 970 cm⁻¹ has been explained in terms of a cavity mode [3].

II. Experimental results

A series of PSC films were fabricated from bulk, *n*-type substrates (*n*-PSC) of both 6H and 4H SiC polytypes ($N_D \sim 10^{18}$ cm⁻³) and from *p*-type 6H-SiC substrates (*p*-PSC) ($N_A \sim 10^{18}$ cm⁻³). For the series of data shown in Fig. 1, an *n*-PSC film was formed in *n*-type 4H-SiC. Spectra taken from samples from different areas of this film were nearly identical, and the samples were subsequently exposed to different lengths of time of brief oxidation. Upon oxidation, the *reststrahlen* band narrows (decreasing at high frequencies) and changes shape, and a peak at ~ 1100 cm⁻¹, not seen

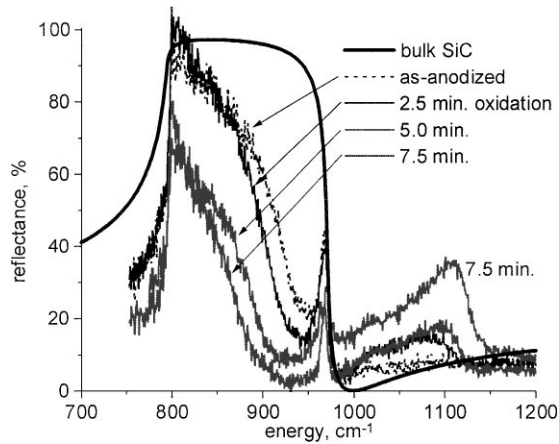


Figure 1. IR reflectance from bulk 4H-SiC, as-anodized PSC, and effects of brief oxidation on *n*-PSC reflectance.

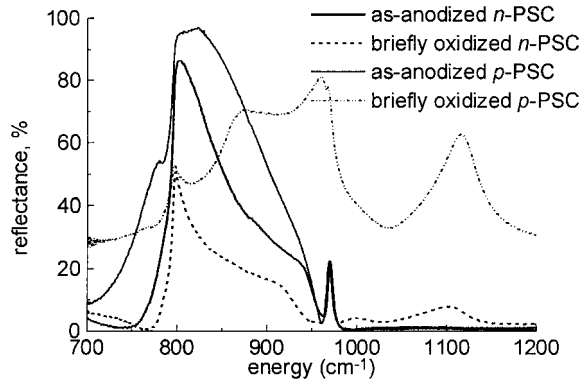


Figure 2. As-anodized and passivated *n*-PSC and *p*-PSC from 6H-SiC.

in bulk SiC and presumably due to SiO₂, becomes more prominent. A second peak at 1016 cm⁻¹ is seen after the anodizations, and more prominently, after oxidation; it disappears after rinsing the samples in ethanol.

Similar experiments were conducted films of *p*-PSC and *n*-PSC films prepared with 6H-SiC substrates. The corresponding spectra for each of the *n*-PSC samples are qualitatively similar to those for *n*-PSC formed from 4H material. The spectra of oxidized *p*-PSC samples are, however, quite different from those for the *n*-PSC samples; in particular the reststrahlen band is nearly gone and the SiO₂ peak is quite strong. Representative spectra are shown in Fig. 2. The observation that the change in reflectance of *n*-PSC due to thermal oxidation is small, while the change for *p*-PSC is more pronounced, can be understood in terms of the differences in the size of the nanostructures in *n*-PSC

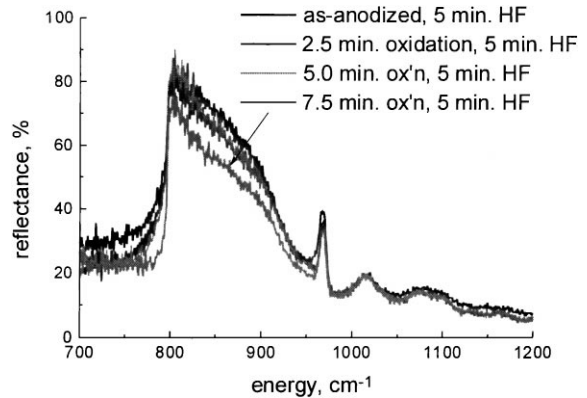


Figure 3. *n*-PSC reflectance following oxide removal.

and *p*-PSC prior to oxidation. Essentially, in 5 min, an appreciably large portion (if not all) of the crystallite of *p*-PSC is consumed by oxidation (on the basis of available oxidation rate data of 4H-SiC and 6H-SiC [4]), whereas the same exposure of an *n*-PSC sample results in the conversion of only a small fraction of the crystallite to oxide.

Following oxidation, one of each of three pairs of samples prepared from 4H-SiC was briefly placed in a solution of 49% HF to etch the oxide. The reflectance of each sample was then measured, which is shown in Fig. 3, along with the spectra from the as-anodized film. Following the HF treatment, the reststrahlen band broadens, but not to the width before oxidation, and the peak near 1100 cm⁻¹ gets smaller (see Fig. 1); this broadening is most pronounced for samples oxidized for the longest time.

III. MODEL

Since the wavelength of light is much larger than the characteristic features of PSC (e.g. pore diameter, interpore spacing), the reflectance from PSC in the reststrahlen band can be understood by modeling the dielectric function of PSC in terms of an effective medium theory. MacMillan, et al. [3] demonstrated that the cavity Maxwell-Garnett model (C-MG), which consists of spherical cavities of air ($\epsilon_{\text{air}} = 1$) surrounded by bulk SiC, accounts reasonably well for the general features of the PSC reststrahlen band. The SiC was characterized as a Lorentzian polarizable medium having TO and LO phonon frequencies, a high-frequency dielectric constant, and a damping parameter. It will be shown in a future publication that the C-MG model

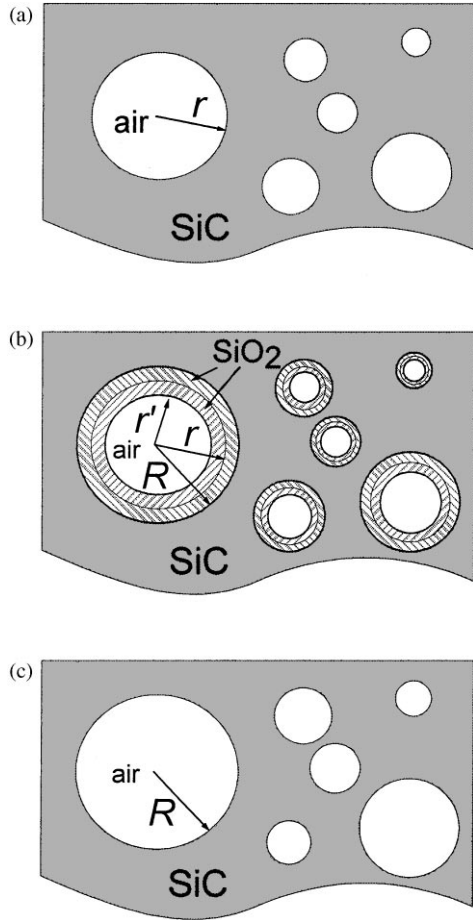


Figure 4. (a) As-anodized PSC. (b) Oxidized PSC. (c) After removal of SiO_2 .

does not characterize many features of as-anodized and non-oxidized PSC quantitatively, and needs to be modified. Still, with one modification it does at least characterize the oxidation of PSC qualitatively.

The infrared reflectance spectrum is modeled at three process stages: (1) after the initial formation of the PSC film (anodization), (2) after a short thermal oxidation of the PSC film, and (3) after etching of the oxide in HF, as shown in Figs. 4(a–c). For simplicity, we assume that the pores are spherical. The radius of a typical pore is defined to be r . This system of air cavities is the C-MG model used in Ref. [3] and is used to model as-anodized PSC. During oxidation, SiC in the spherical shell from radius r to R is converted to oxide. Since the ratio of the molar volume of SiO_2 to that of SiC, g , exceeds one ($g = 2.11$), the radius of the pore decreases to r' as a result of oxidation, where $r'^3 = R^3 - (R^3 - r^3)g$. The dielectric function for such a configuration is expressed

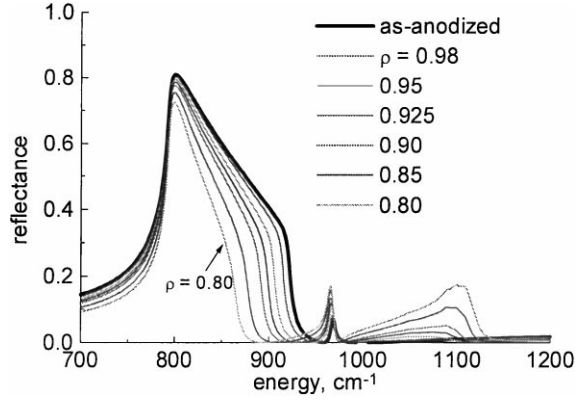


Figure 5. Simulated reflectance after oxidation, hybrid model, infinite half-space PSC (stage 2).

in terms of the dielectric functions of air, oxide [5] and SiC, and the volume fraction of each in a manner based on [6]:

$$\varepsilon_{\text{PSC}}(\omega) = \frac{f' A \rho^3 + f' \varepsilon_{\text{SiO}_2} B (1 - \rho^3) + \varepsilon_{\text{SiC}} (1 - f')}{f' A \rho^3 + f' B (1 - \rho^3) + (1 - f')} \quad (1)$$

where f' is the volume fraction of air and SiO_2 , $\varepsilon_{\text{SiO}_2}(\omega)$ is the frequency-dependent complex dielectric function of SiO_2 , $\rho = r'/R$, and A and B are functions of $\varepsilon_{\text{SiC}}(\omega)$ and $\varepsilon_{\text{SiO}_2}(\omega)$. (The effect of strain in the oxide is ignored in this model.)

We have modeled the reflectance following anodization, oxidation, and oxide removal from both semi-infinite PSC films and PSC films-on-bulk SiC using the C-MG model as described above, and also by hybridizing the C-MG model with the LLL effective medium model [7] for the case of an infinite halfspace of PSC. In both the C-MG and the new hybrid model, the course of oxidation is expressed as a decreasing value of a parameter $\rho = r'/R$, where $\rho = 1$ corresponds to the as-anodized sample (containing no SiO_2). Both models reveal a narrowing of the reststrahlen band width. While the modified C-MG model results (not shown) are qualitatively consistent with the data in Fig. 1, the hybrid model, shown in Fig. 5, produces the shape of the reststrahlen band much better. Both models show the appearance of the antisymmetric Si–O stretching mode near 1100 cm^{-1} , which is also observed in the data. In the simulation corresponding to stage 3 using the hybrid model, in which the oxide layers have been removed, the model results shown in Fig. 6 are in good

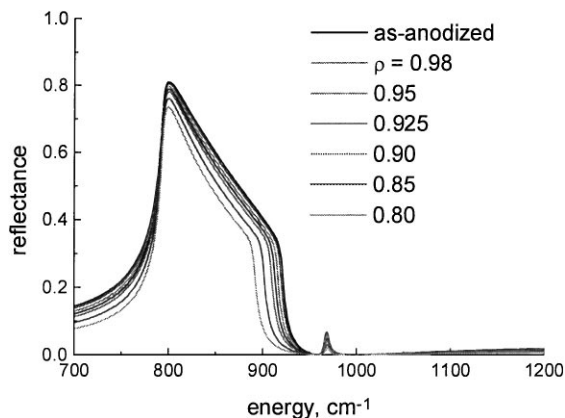


Figure 6. Simulated reflectance after oxide removal, hybrid model, infinite half-space PSC (stage 3).

agreement with the data shown in Fig. 3, including the increase in the reflectance of the reststrahlen shoulder on the high-frequency side.

IV. Concluding Remarks

FTIR reflectance is shown to be sensitive to changes in the PSC composition resulting from a brief thermal oxidation. These changes are more striking for *p*-PSC than for *n*-PSC. These results are indicative of the differences in the nanostructure of the pre-oxidation material in *n*-PSC and *p*-PSC. When the C-MG model is extended to support an interfacial oxide layer between the pore and the surrounding SiC, it qualitatively reproduces the general trends observed in experimental data, but does not simulate the shape of the reststrahlen band well. A new hybrid effective medium model using

the C-MG and Looyenga models has given quantitative agreement with experiment. This model may be capable of determining PSC film thickness, porosity, and oxide thickness, and provides an improved description of the microstructural topology of PSC.

Acknowledgments

The authors are grateful to Dr. Luis Avila of the Chemistry Department at Columbia for kindly permitting us use of the FTIR spectrometer. We also wish to acknowledge the financial support of Dr. Anthony D. Kurtz and Kulite Semiconductor Products, Inc. in Leonia, NJ, and the Joint Services Electronics Program, Contract No. DAA-G55-97-1-0166.

References

1. L. Tsybeskov, S.P. Duttagupta, and P.M. Fauchet, *Solid State Comm.* **95**, 429 (1995).
2. J.E. Spanier, G.S. Cargill III, I.P. Herman, S. Kim, D. Goldstein, A.D. Kurtz, and B.Z. Weiss, in *Advances in Microcrystalline and Nanocrystalline Semiconductors-1996*, edited by R.W. Collins, P.M. Fauchet, I. Shimizu, J.-C. Vial, T. Shimada, and A.P. Alivisatos (Mat. Res. Soc. Symp. Proc. **452**, Pittsburgh, PA, 1997), p. 491.
3. M.F. MacMillan, R.P. Devaty, W.J. Choyke, J.E. Spanier, D. Goldstein, and A.D. Kurtz, *J. Appl. Phys.* **80**, 2412 (1996).
4. Z. Zheng, R.E. Tressler, and K.E. Spear, *J. Electrochem. Soc.* **137**, 854 (1990).
5. H.R. Philipp, in *Handbook of Optical Constants of Solids*, edited by E.D. Palik (Academic Press, New York, 1985), p. 762.
6. J.H. Weaver, R.W. Alexander, L. Teng, R.A. Mann, and R.J. Bell, *Phys. Stat. Sol. A* **20**, 321 (1973).
7. H. Looyenga, *Physica* **31**, 401 (1965); Landau-Lifshitz, *Lehrbuch der theoretischen Physik, Band VIII: Elektrodynamik der Kontinua* (Akademie-Verlag, Berlin, 1967), p. 55.